43rd AIAA/ASME/SAE/ASEE Joint Propulsion Conference & Exhibit
8 - 11 July 2007, Cincinnati, OH

AIAA 2007-5618

Neutronics Models and Analysis of the Small Nuclear Rocket Engine (SNRE)

Bruce G. Schnitzler*
NASA Glenn Research Center, Cleveland, OH, 44135
Intergovernmental Personnel Act (IPA) Assignee from Idaho National Laboratory

and

Stanley K. Borowski†
NASA Glenn Research Center, OH,44135

The fundamental goal of the President's Vision for Space Exploration announced in early 2004 is to advance U.S. scientific, security, and economic interest through a robust space exploration program. Human expeditions to Mars were one of the long-term activities identified in support of this goal. Although mission architecture, schedule, and preferred hardware have not yet been identified, crewed exploration missions will demand exceptional propulsion system performance. Past studies, in particular those in support of both the Strategic Defense Initiative (SDI) and Space Exploration Initiative (SEI), have shown nuclear thermal propulsion systems provide superior performance for high mass high propulsive delta-V missions. An extensive nuclear thermal rocket technology development effort was conducted from 1955-1973 under the Rover/NERVA Program. The Small Nuclear Rocket Engine (SNRE) was the last engine design studied by the Los Alamos National Laboratory during the program. At the time, this engine was a state-of-the-art design incorporating lessons learned from the very successful technology development program. Recent activities at the NASA Glenn Research Center have included upgrading and modernizing nuclear thermal propulsion system models and analysis methods. A highly detailed MCNP Monte Carlo transport model based on the SNRE was developed as a computational benchmark. Several simpler MCNP models were also developed and exercised. Results from the simpler models are compared to the benchmark model results and to available documentation for the SNRE. Results comparisons include engine reactivity (k-effective), control system reactivity worth, engine system energy balances, core interior component heating, and relative MCNP execution times.

Nomenclature

k-eff	=	effective multiplication factor
K	=	temperature (Kelvin)
lbf	=	thrust
ENDF/B	=	Evaluated Nuclear Data File
MCNP	=	Monte Carlo N-Particle transport code
MWth	=	thermal power
NTP	=	Nuclear Thermal Propulsion
NEDS	=	Nuclear Engine Definition Study
NERVA	=	Nuclear Engine for Rocket Vehicle Applications
SNRE	=	Small Nuclear Rocket Engine

* INL Staff Member, Space Nuclear Systems Division, 21000 Brookpark Road, MS 77-5, AIAA Senior Member.
† Lead Engineer, Nuclear Thermal Propulsion Systems, 21000 Brookpark Road, MS 77-5, AIAA Associate Fellow.

I. Introduction

The fundamental goal of the President's Vision for Space Exploration[1] is to advance U.S. scientific, security, and economic interest through a robust space exploration program. Eventual human expeditions to Mars were one of the long-term activities identified in support of this goal. Although mission architecture, schedule, and preferred hardware have not yet been established, crewed exploration missions will demand exceptional propulsion system performance. Past studies, in particular those in support of both the Strategic Defense Initiative (SDI) and the Space Exploration Initiative (SEI), have shown nuclear thermal propulsion systems provide superior performance for high mass high propulsive delta-V missions.

Recent activities at the NASA Glenn Research Center have included upgrading and modernizing nuclear thermal propulsion system models and analysis methods. Initial efforts have been focused on benchmarking methods and models against the Small Nuclear Rocket Engine (SNRE) documented in the Nuclear Engine Definition Study (NEDS) Preliminary reports[2,3] This paper addresses neutronics modeling. A companion paper[4] addresses integrated thermal-fluid-structural analysis of reactor core interior components. Results from both the neutronics and integrated thermal-fluid-structural analyses are used to confirm and upgrade the NESS[5] engine system level analysis code.

II. Small Nuclear Rocket Engine (SNRE)

The primary reasons for selecting the SNRE for analysis are the maturity of the engine design, the engine size and thrust level, and the quality of the available documentation. The SNRE is the last engine design studied by the Los Alamos National Laboratory during the Rover Program and incorporates lessons learned throughout the very successful technology development program. Although the program was terminated prior to completion of the design, available preliminary design results provide reasonably good documentation, especially for the reactor core. The SNRE also provides a valuable small engine analytic benchmark for propulsion systems in a lower thrust range of potential interest.

Design requirements for the small engine included the ability to operate at either of two full power conditions. Full power operating conditions for a single-mission injection mode are one-hour engine life at 367 MWth yielding 16,406 lbf thrust with a specific impulse of 875 seconds. Full power conditions for operation in a reusable mission mode are two-hour engine life at 354 MWth yielding 16,125 lbf thrust with a specific impulse of 860 seconds. Engine specific impulse is a function of several parameters including propellant molecular weight, propellant temperature, and nozzle expansion ratio. The SNRE nozzle expansion ratio of 100:1 was established primarily by the requirement that the stage be carried into earth orbit by the then planned space shuttle. Hydrogen propellant chamber temperatures are 2696 K and 2633 K, respectively, for the two operating modes.

The engine utilizes hexagonal fuel elements and hexagonal structural support or "tie tube" elements. Both element types are 1.905 cm (0.750 in) across the flats and 89 cm (35 in) in length. The fuel composition is the (U,Zr)C-graphite "composite" described by Taub[6] and successfully tested in the Nuclear Furnace 1 test reactor.[7] The regeneratively cooled tie tube elements provide structural support for the fuel elements, provide a source of energy to drive the turbomachinery, and incorporate a zirconium hydride moderator sleeve to raise neutronic reactivity in the small engine size. The core contains 564 fuel elements and 241 tie tube elements. Additional complete and partial hexagonal elements of beryllium "filler" elements are utilized to complete an approximately cylindrical core.

The reference SNRE engine design was based on composite fuel with a (U,Zr)C solid solution content of 35% by volume. In the initial design effort, evaluations were first performed with a uniform uranium loading of 0.64 g/cm^3. Element uranium loadings were then selectively reduced in the higher power elements to flatten the radial fission profile across the core.

The reactor core cross section at the axial mid-plane is illustrated in Fig. 1. This particular cross section is from a geometric model described in a later section. In this figure, the interior details of the tie tube elements and the propellant channels in the fuel elements are omitted for clarity. The tie tube elements are shown as yellow hexagons with an inner green circle and fuel elements are shown as open red hexagons. Peripheral core components include a stainless steel membrane, a beryllium barrel located between the filler elements and a beryllium reflector, and an aluminum alloy pressure vessel. Reactivity control is provided by twelve cylindrical control drums located in the radial reflector. The rotating drums contain neutron absorber plates over a 120-degree sector of their outer surface.

A lower tie tube plenum, support plate, and upper tie tube plenum are located immediately forward of the active core region. Radiation shielding is provided by a borated zirconium hydride shield assembly just forward of the upper tie tube plenum. An optional annular brim shield is positioned just forward of the drum actuator zone. A core longitudinal cross section is shown in Fig. 2. Additional dimensional data are provided in the appendix. Material compositions are described in Table III-I of Ref. 3.

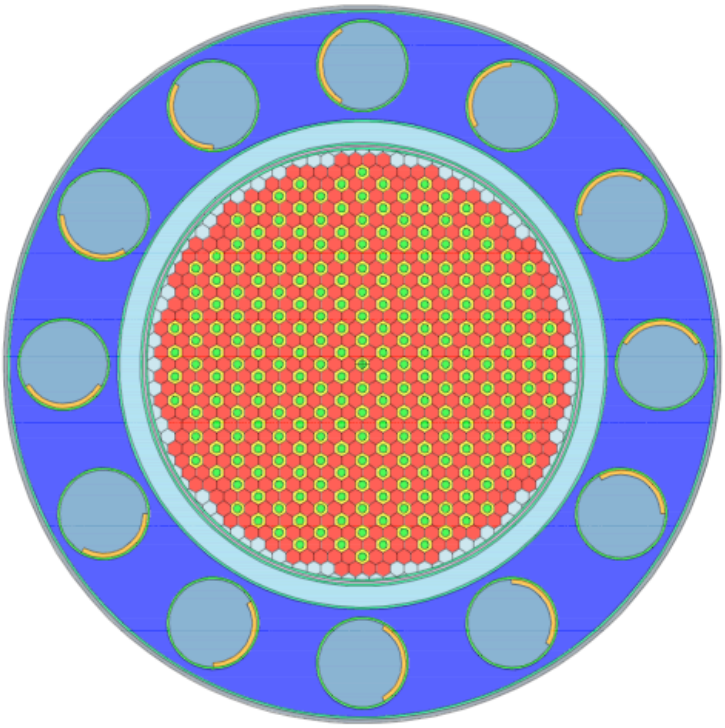

Figure 1. SNRE MCNP model cross section at core mid-plane.

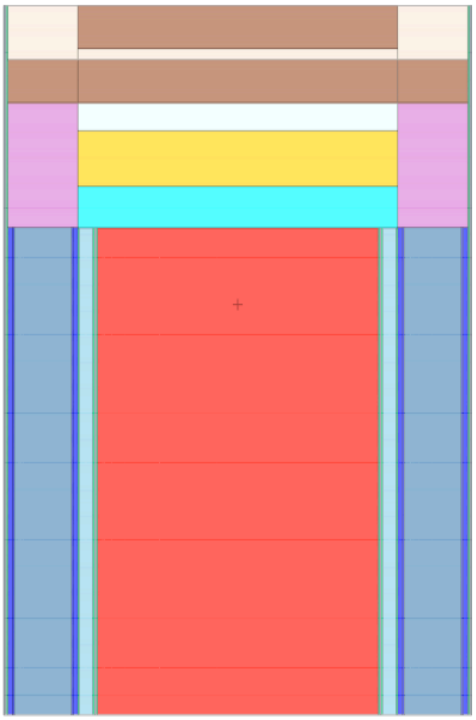

Figure 2. SNRE MCNP model vertical cross section through core centerline.

III. Analysis Methods

Historically, a variety of analytic methods have been utilized in the design and performance evaluations of nuclear thermal propulsion systems. The most important have been Monte Carlo, one-dimensional and multi-dimensional discrete ordinates transport, and point-kernel methods. The selection of both analytic methods and the level of modeling detail to be employed are influenced by several factors including model development time, available computational capacity, and the intended application of the results. Lower fidelity solutions may often suffice for some scoping studies such as preliminary engine sizing. At the other end of the spectrum is the reactor equivalent of modern aircraft design where a vehicle may be flown computationally as an integral part of the design process.

All transport evaluations reported here were performed using the MCNP Monte Carlo transport code.[8] Cross section data employed in the MCNP transport calculations are primarily from the Evaluated Nuclear Data File[9,10] (ENDF/B) Versions V and VI. The ENDF/B cross section evaluations for some materials of interest, in particular the zirconium and hafnium isotopes, do not include photon yield data. The ENDF/B evaluations were employed for estimating core reactivity and alternate Lawrence Livermore evaluations[11] for some materials substituted for energy deposition evaluations.

IV. MCNP Models

All MCNP models employed include the reactor core and the radial components outward through the pressure vessel wall. The models extend axially from the aft end of the active fuel forward through the internal shields. The pressure vessel forward dome and the regions aft of the active fuel, including the nozzle, were not modeled. The hydrogen tank and miscellaneous hardware components, such as the turbine, hydrogen propellant turbopump, and propellant piping, were not modeled. Although the omitted components will clearly impact external radiation fields, all analyses and results described here are focused on the reactor interior. The radial and axial components external to the reactor core are common to all evaluations. Geometry data for the external components are included in the appendix.

The reactor core was modeled at six different levels of detail. Model features are summarized in Table 1.

Composite fuel elements are 1.905 cm (0.750 in) across the flats and 89 cm (35 in) in length. Fuel elements contain 19 propellant coolant channels with a 0.25654-cm (0.101-in) borehole diameter. The borehole pitch is 0.40894 cm (0.161 in). The hexagonal outer surfaces are coated with a 50 micrometer thick ZrC protective layer. The actual interior borehole coating thickness increases gradually from about 50 micrometer at the inlet to about 150 micrometer at the outlet end. A uniform 100 micrometer thickness is assumed for the MCNP models.

Tie tube elements are also 1.905 cm across the flats and 89 cm in length. The tie tube geometry cross section is shown in Fig. 3. Tie tube radial regions and dimensions are shown in the appendix.

The fuel element and tie tube element pattern in the interior of the reactor core is illustrated in Fig. 4.

Table 1. Small Nuclear Rocket Engine core models.

Reactor Core Model Features
Explicit Lattice
Explicit Models of Fuel Element Components
Explicit Models of Tie Tube Element Components
564 Fuel + 241 Tie Tube + 120 Filler Elements [MCNP Lattice Feature]
Homogenized Lattice
Homogenized Fuel Element Compositions
Homogenized Tie Tube Element Compositions
564 Fuel + 241 Tie Tube + 120 Filler Elements [MCNP Lattice Feature]
Homogenized Discrete
Homogenized Fuel Element Compositions
Homogenized Tie Tube Element Compositions
Discrete Models of 564 Fuel + 241 Tie Tube + 120 Filler Elements
Homogenized 18-Zone
Homogenized Element Compositions
18 Zones – Central Cylindrical Plus 17 Annular
One Radial Zone for Each Successive Hexagonal Row of Elements
Homogenized Two Zone
Homogenized Element Compositions
Two Zones – Central Cylindrical Plus One Annular
Inner Zone Representing 420 Fuel + 211 Tie Tube Elements
Outer Zone Representing 144 Fuel + 30 Tie Tube + 120 Filler Elements
Homogenized Single Zone
Homogenized Element Compositions
Single Cylindrical Zone
One Zone Representing 564 Fuel + 241 Tie Tube + 120 Filler Elements

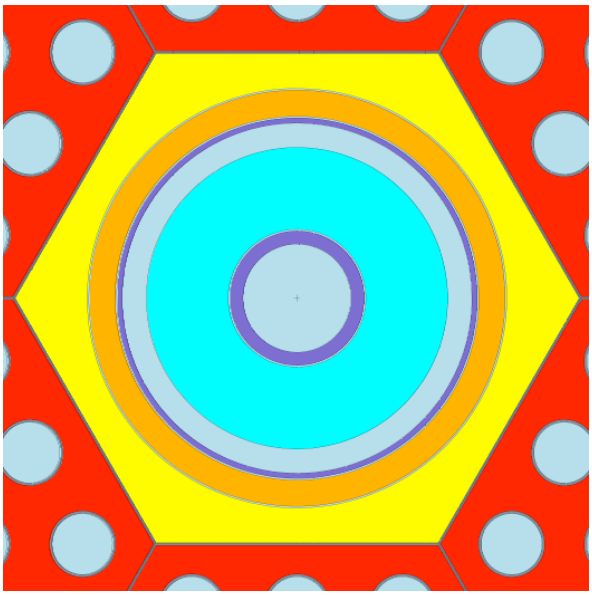

Figure 3. Tie tube element cross section.

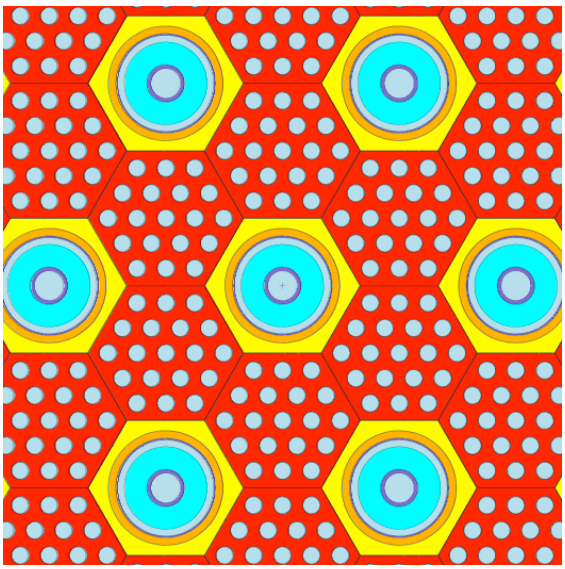

Figure 4. Fuel element – tie tube element pattern in core interior.

The composite fuel matrix baseline composition employed for all MCNP calculations closely matches that shown in Table I of Ref. 7. The fuel matrix bulk density is 3.64 g/cm^3 and contains 0.60 g/cm^3 uranium, 1.23 g/cm^3 carbon, and 1.81 g/cm^3 zirconium. The uranium is highly enriched to 93 weight percent U-235. All reported evaluations were performed assuming uniform uranium enrichment and uniform fissile loading. These conditions correspond to the initial evaluations performed during the SNRE design process just prior to fuel zoning to flatten radial power distributions.

The Explicit Lattice model is the most highly detailed and serves as the computational benchmark. The model consists of a single hexagonal tie tube model as described above and shown in Fig. 3, a single hexagonal fuel element model as described above, and a single hexagonal beryllium filler model. The three hexagonal element models all have identical exterior dimensions. The MCNP lattice feature is used to propagate the three element types and completely fill the reactor core region.

The Homogenized Lattice model is similar except the fuel element and tie tube element models both consist of a single "homogenized" zone. The zone material composition is established by volume weighting the material compositions of the element components. The MCNP lattice feature is again used to propagate the three element types and completely fill the reactor core region. Models of this type typically provide faster running times but sacrifice interior detail such as tie tube component heating rates.

The Homogenized Discrete model consists of 564 fuel elements, 241 tie tube elements, and 120 complete or partial beryllium filler elements. Homogenized material compositions, identical for each element type, are employed, but each element is individually constructed using six exterior surfaces making up the faces of the hexagonal element plus the aft and forward surfaces. This model was developed to facilitate subsequent fuel zoning and depletion analyses. Given the same homogenized compositions for each of the element types, results from the Homogenized Lattice and Homogenized Discrete models should be identical within Monte Carlo statistical errors.

The Homogenized 18-Zone model consists of a cylindrical zone at the core centerline plus 17 annular zones. The central cylindrical zone represents the central tie tube element. Each successive annular zone represents each successive row of hexagonal elements. Zone radial dimensions are established by conserving the total volume of the hexagonal elements in the row. Zone compositions are established by volume weighting on the number of element types in the row. A different, but not described, radial zoning scheme was used in Ref. 3.

The Homogenized Two Zone and Homogenized Single Zone models consist of zones with dimensions and compositions established using the same schemes as for the 18-Zone model. The Two Zone model inner zone represents the first fifteen hexagonal rows of elements. Again, a different but not described radial zoning scheme was used in Ref. 3.

V. Results

Monte Carlo results are generally reported in the form of a best estimate and a relative error. The range defined by Value = Best Estimate $\pm$ [(Best Estimate) x (One Relative Error)] can be expected to contain the "true" value about 68% of the time. The range defined by Value = Best Estimate $\pm$ [2 x (Best Estimate) x (One Relative Error)] can be expected to contain the "true" value about 95% of the time.

A. Engine Reactivity

Calculated effective multiplication factors (k-eff) for the SNRE models are shown in Table 2. For all cases the control drums are positioned at the 90-dgeree middle-of-range position. The Explicit Lattice model with depletion cross sections is the highest fidelity case. Changes from this base case are reported in dollars assuming an effective delayed neutron fraction of 0.0075. Reactivity differences between the Explicit Lattice and Homogenized Lattice models are statistically significant at the 95% confidence level. Reactivity differences between the Homogenized Lattice and Homogenized Discrete models are not statistically significant. With the exception of the Explicit Lattice model, reactivity values calculated using the heating cross section sets are approximately 0.4 dollars higher than those using the depletion cross section sets. The simpler radial zone models overestimate reactivity by 1 to 2 dollars.

B. Control System Reactivity Worth

The SNRE design featured twelve control drums with boron-copper control plates but the drum design was not complete. Results from two-dimensional (r,θ) calculations had indicated a control drum worth of approximately 8.9 dollars and this was judged adequate. For the MCNP models, absorber plates of 0.635-cm thick hafnium were assumed. The hafnium segment has an inner radius of 5.3975 cm (2.125 in) and extends over a 120-degree sector.

Calculated full range control drum worths are shown in Table 3. With either cross section set, differences among the first three model types are not statistically significant.

The radial zone models all yield overestimated drum worths. The 18-zone models are about 5% high and the one and two zone models are about 7% high compared to the Explicit Lattice model.

Control drum swing worths calculated using the heating cross section sets are all low compared to those calculated using the same core model with the depletion cross section sets.

The calculated control swing of about 11.2 dollars exceeds the 8.9 dollars judged adequate for the SNRE engine design. Reducing the hafnium thickness will both reduce the total control swing worth and will raise the engine reactivity slightly. Preliminary estimates indicate a hafnium absorber thickness of 0.19 cm (0.075 in) will provide a control swing of about 9 dollars. For consistency, the original thicker absorber plate was retained for all models.

Table 2. Calculated effective multiplication factors (k-effective) for SNRE models.

	Depletion Cross-Sections		Heating Cross-Sections	
Model	**Calculated k-effective***	**Change From Base ($)**	**Calculated k-effective***	**Change From Base ($)**
Explicit Lattice	1.001605	Base Case	1.001529	-0.0101
Homogenized Lattice	1.001931	0.0435	1.005417	0.5083
Homogenized Discrete	1.001865	0.0347	1.005225	0.4827
Homogenized 18-Zone	1.006559	0.6605	1.009809	1.0939
Homogenized Two Zone	1.010811	1.2275	1.014365	1.7013
Homogenized One Zone	1.013461	1.5808	1.016479	1.9832

* Relative error for all calculated k-effective values is $\leq$0.00009 ($0.0120)

Table 3. Calculated control drum worth for SNRE models.

	Depletion Cross-Sections		Heating Cross-Sections	
Model	**Full Swing Drum Worth ($)**	**Change From Base ($)**	**Full Swing Drum Worth ($)**	**Change From Base ($)**
Explicit Lattice	11.2247	Base Case	10.8703	-0.3544
Homogenized Lattice	11.1955	-0.0292	10.8881	-0.3365
Homogenized Discrete	11.2255	0.0008	10.8624	-0.3623
Homogenized 18-Zone	11.8109	0.5863	11.4900	0.2653
Homogenized Two Zone	12.0059	0.7812	11.6791	0.4545
Homogenized One Zone	12.0593	0.8347	11.6756	0.4509

Relative error for all calculated k-effective values is $\leq$0.00009 ($0.0120)

C. Engine System Energy Balances

Calculated engine system energy balances are shown in Table 4. All energy deposition and leakage data are from models using heating cross section sets. Sufficient particle histories were utilized to reduce maximum relative errors to $\leq$0.0005 in the listed core and radial components and to $\leq$0.0027 in the listed forward components. There are no statistically significant differences observed among the six models.

Photons produced by neutron interactions are available for transport and normally result in both local and remote energy deposition. For those materials without photon yield data, the photon energy that would have been available is assumed to be deposited at the site of the neutron interaction. Although energy balance results obtained using the depletion cross section sets are not tabulated here, some qualitative observations are appropriate.

For the SNRE engine models, use of the depletion cross section sets would result in overestimating energy deposition in the hafnium absorber plates by a factor of about 2.76 (~4.35 MW as opposed to ~1.58 MW). Use of

the depletion sets would also underestimate energy deposition in some components. In particular, deposition in the pressure vessel and in the control drum beryllium bodies would be underestimated by as much as a factor of two. Radial photon energy leakage would also be underestimated by about a factor of two.

Table 4. Calculated energy balances in SNRE MCNP models.

	Component Heating Fraction					
Region	Explicit Lattice	Homogenized Lattice	Homogenized Discrete	Homogenized 18-Zone	Homogenized Two Zone	Homogenized One Zone
Fuel elements	0.94809	0.94793	0.94789			
Tie tube elements	0.01915	0.01936	0.01937			
Be filler elements	0.00224	0.00224	0.00224			
Core total	0.96948	0.96953	0.96950	0.96949	0.96950	0.96940
Radial gap	0.00002	0.00002	0.00002	0.00002	0.00002	0.00002
Stainless wrapper	0.00164	0.00164	0.00164	0.00166	0.00168	0.00169
Radial gap	0.00002	0.00002	0.00002	0.00002	0.00002	0.00002
Be barrel	0.00386	0.00386	0.00386	0.00395	0.00399	0.00407
Radial gap	0.00001	0.00001	0.00001	0.00001	0.00001	0.00001
Radial Be reflector	0.00609	0.00608	0.00609	0.00613	0.00614	0.00621
Radial gap	0.00000	0.00000	0.00000	0.00000	0.00000	0.00000
Pressure vessel	0.00033	0.00033	0.00033	0.00033	0.00033	0.00033
Control absorbers	0.00445	0.00445	0.00445	0.00440	0.00438	0.00437
Control drum Be	0.00331	0.00331	0.00331	0.00332	0.00332	0.00335
Control drum hydrogen	0.00001	0.00001	0.00001	0.00001	0.00001	0.00001
Lower tie tube plenum	0.00016	0.00016	0.00016	0.00016	0.00015	0.00010
Support plate	0.00031	0.00031	0.00031	0.00030	0.00030	0.00030
Lower tie tube plenum	0.00010	0.00010	0.00010	0.00010	0.00010	0.00010
Lower internal shield	0.00110	0.00108	0.00109	0.00107	0.00106	0.00104
Hydrogen zone	0.00000	0.00000	0.00000	0.00000	0.00000	0.00000
Upper internal shield	0.00018	0.00018	0.00018	0.00018	0.00018	0.00017
Drum actuator zone	0.00019	0.00019	0.00019	0.00019	0.00019	0.00019
Brim Shield	0.00057	0.00056	0.00056	0.00056	0.00055	0.00055
Hydrogen zone	0.00000	0.00000	0.00000	0.00000	0.00000	0.00000
Radial neutron leakage	0.00077	0.00077	0.00077	0.00078	0.00077	0.00079
Aft neutron leakage	0.00073	0.00073	0.00073	0.00071	0.00070	0.00068
Forward neutron leakage	0.00003	0.00003	0.00003	0.00003	0.00003	0.00003
Radial photon leakage	0.00548	0.00548	0.00548	0.00543	0.00542	0.00542
Aft photon leakage	0.00109	0.00108	0.00109	0.00108	0.00108	0.00108
Forward photon leakage	0.00007	0.00007	0.00007	0.00007	0.00007	0.00007

D. Core Interior Energy Deposition Distribution.

Total energy deposition rates in each fuel element and in each tie tube element are available from the Explicit Lattice, Homogenized Lattice, and Homogenized Discrete models. No statistically significant differences in calculated heating rates for particular elements are observed among these three models.

Local energy deposition peaking can be quantified in terms of a heating rate ratio for fuel element n defined as H_n = (total heating in element n) x (total number of fuel elements) / (total heating in all fuel elements). A similar heating rate ratio is defined for the tie tube elements.

Relative energy deposition rates from the Homogenized Discrete model prior to fuel zoning and with all control drums at middle of range (90-degree) positions are illustrated in Fig. 5. Element hexagons are color coded with red, light blue, and green representing fuel elements and orange, yellow, and violet represent tie tube elements. Beryllium filler elements and partial elements at the core periphery are dark blue.

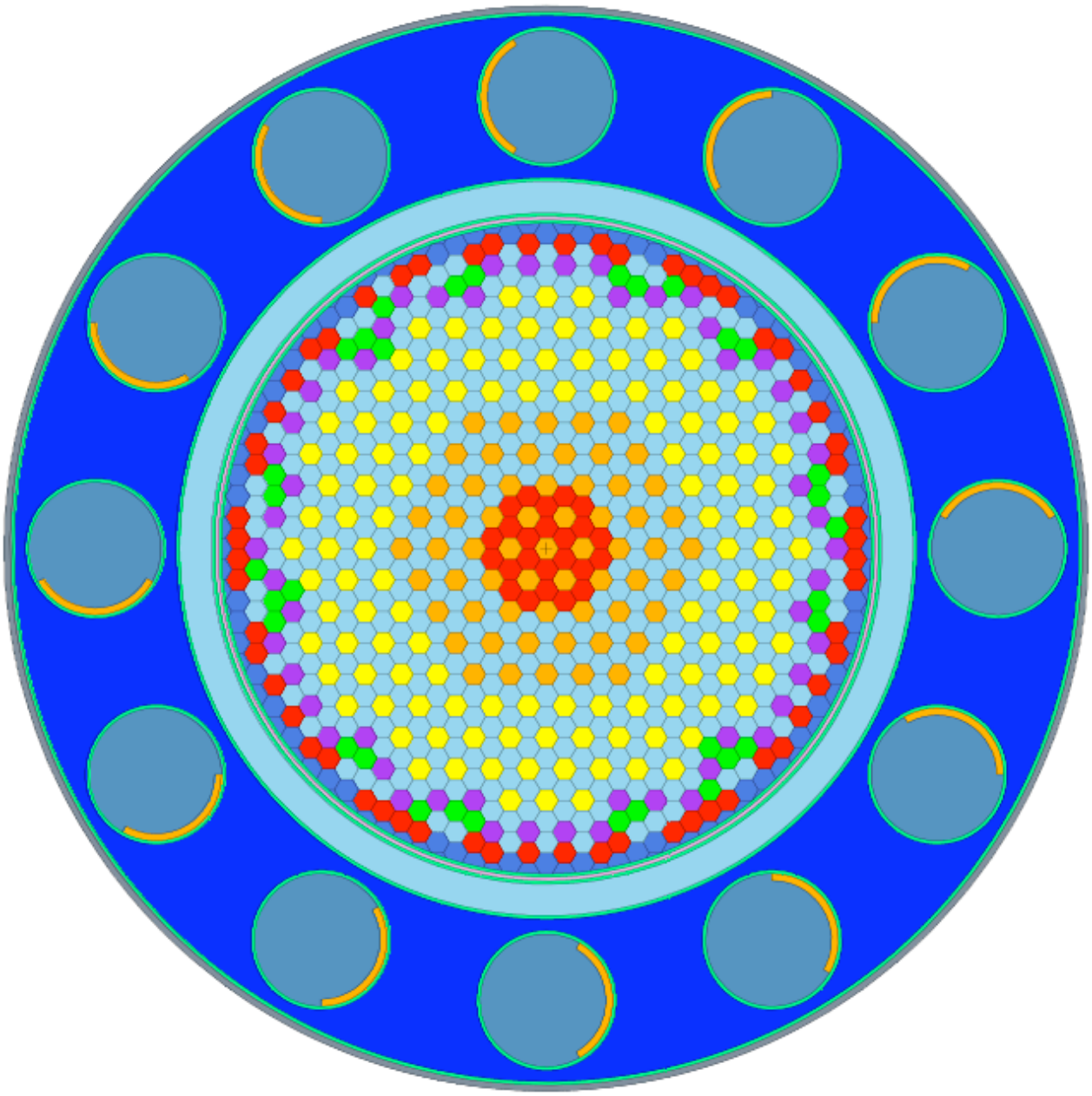

Figure 5. Relative heating in SNRE core with uniform fuel loading and all control drums at 90-degrees.

Fuel elements operating within ±10% of the average fuel element power are shown in light blue. Fuel elements operating at greater than 110% of the average fuel element power are shown in red. Fuel elements operating at less than 90% of the average fuel element power are shown in green. Tie tube elements within ±10% of the average tie tube element energy deposition are shown in yellow. Warmer (>110%) and cooler (<90%) tie tube elements are shown in orange and violet, respectively.

Fuel element heating is peaked slightly (about 112%) at the center of the core and more sharply at the core periphery near the beryllium barrel and reflector. The maximum fuel peaking at the core periphery is about 130%. The core heating pattern is quite symmetric with minor perturbations produced by the control drum absorbers.

Preliminary evaluations indicate very flat radial power profiles will be achievable via element enrichment zoning with 551 of the 564 fuel elements within 1% of the average. Heating rates in the remaining 13 elements range from 96.6% to 99% of the average.

E. Fuel and Tie Tube Element Component Energy Deposition

High fidelity integrated thermal-fluid-structural analyses of particular fuel elements and particular tie tube elements or combinations of elements requires spatially resolved energy deposition rates in each component. Heating rate tally sets in the Explicit Lattice model are available for short axial segments of each component. Although the axial segment length is somewhat arbitrary, a 1-cm spacing is currently employed. Segment heating data may be used directly or the total heating in each component may be used along with an axial heating profile. Table 5 lists heating fractions for each component of the fuel and tie tube elements. A representative axial heating profile is shown in Fig. 6. The Table 5 values are averaged over all core elements of that particular type and the Fig. 6 profile is averaged over the fuel matrix of all fuel elements.

The Table 5 and Fig. 6 data are calculated using the heating cross section sets. For this SNRE Explicit Lattice model, use of the depletion cross section sets would overestimate energy deposition in the ZrC clad and in the ZrH moderator by about 7% and by about 6%, respectively. Deposition in the Inconel-718 tie tubes would be underestimated by about 3%.

Table 5. Fuel and tie tube element component heating fractions.

Component	Fraction of Element Total Heating
Fuel Element	
Fuel matrix	0.99510
Outer element clad	0.00083
Hydrogen propellant	0.00032
Propellant channel clad	0.00375
Tie Tube Element	
Inner hydrogen	0.00108
Inner tie tube	0.04090
Gap hydrogen	0.00008
ZrH moderator	0.57159
Outer hydrogen annulus	0.00299
Outer tie tube	0.04928
Gap hydrogen	0.00023
Insulator tube	0.12383
Gap hydrogen	0.00026
Graphite hexagonal body	0.19190
Outer element clad	0.01786

All relative errors $\leq$0.0002

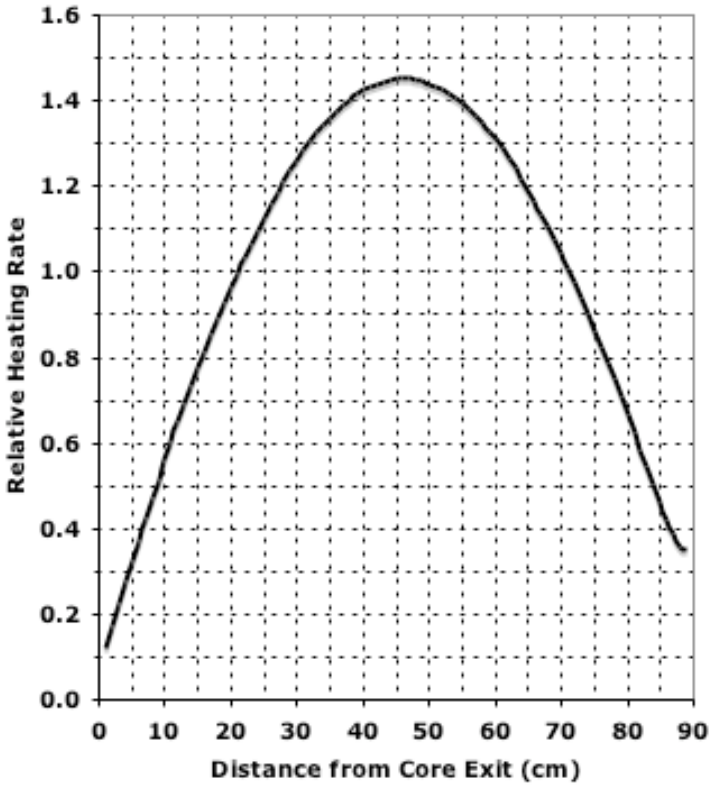

Figure 6. Axial energy deposition profile in fuel matrix.

F. Relative MCNP Execution Times for SNRE Models

Execution times are often important in model selection. Models with complex geometries inevitably require longer execution times to complete a given number of particle histories. In addition, more complex geometry usually means smaller volumes of interest and more particle histories are required to achieve acceptable statistics on the quantities of interest in the smaller volumes. Models using heating cross section sets will run slightly faster than identical models using depletion cross section sets.

The Explicit Lattice models require the longest execution times. The Homogenized Lattice models typically run about four times faster than the Explicit Lattice models. The Homogenized Discrete models run about 2.5 times faster than the Homogenized Lattice models and ten times faster than the Explicit Lattice models. The simpler radial zone models typically run from 15 to 20 times faster than the Explicit Lattice models.

VI. Conclusions

Beginning-of-life core reactivity, control worth, and energy deposition axial profile results obtained using MCNP and the SNRE computational benchmark model are in good agreement with those presented in the SNRE documentation. Element-by-element and radial and axial element component energy balances are not explicitly specified in the SNRE references, but calculated integral results are consistent with the available documentation.

Heating cross section sets are required for all energy deposition evaluations and will also be required for external radiation field evaluations. Depletion cross section sets should be used for any engine reactivity and control system worth evaluations.

The Explicit Lattice model (with heating cross sections) provides spatially resolved individual component energy deposition rates needed for high fidelity integrated thermal-fluid-structural analyses of fuel and tie tube elements. Execution times are acceptable for routine design and analysis use.

Homogenized Element models can be used with confidence for control system worth and engine energy balance evaluations and to support fuel zoning for power flattening.

Results for fuel zoning to flatten radial power distributions, for fuel depletion analyses, and for external radiation fields will be reported in the future.

Appendix

Table 6. Small Nuclear Rocket Engine MCNP model geometry.

Region	Inner Radius (cm)	Outer Radius (cm)	Aft Boundary (cm)	Forward Boundary (cm)
Core		29.5275	0.0	89.0
Gap	29.5275	29.8450	0.0	89.0
Stainless steel wrapper	29.8450	30.1625	0.0	89.0
Gap	30.1625	30.4800	0.0	89.0
Beryllium barrel	30.4800	33.3375	0.0	89.0
Gap	33.3375	33.6550	0.0	89.0
Beryllium radial reflector	33.6550	43.3870	0.0	89.1
Gap	43.3870	48.7045	0.0	129.64
Pressure vessel	48.7045	49.2633	0.0	129.64
Lower tie tube plenum		33.6550	89.000	96.620
Core support plate		33.6550	96.620	106.780
Upper tie tube plenum		33.6550	106.780	111.860
Lower internal shield		33.6550	111.860	119.734
Hydrogen plenum		33.6550	119.734	121.766
Upper internal shield		33.6550	121.766	129.640
Control drum actuator zone	33.6550	48.3870	89.100	111.860
Brim shield	33.6550	48.3870	111.860	119.734
Hydrogen	33.6550	48.3870	119.734	129.640

Table 7. SNRE MCNP model tie tube element geometry.

Component	Material	Inner Radius (cm)	Outer Radius (cm)
Inner hydrogen	Hydrogen		0.20955
Inner tie tube	Inc-718	0.20955	0.26035
Gap	Hydrogen	0.26035	0.26670
Moderator	ZrH	0.26670	0.58420
Gap	Hydrogen	0.58420	0.67818
Outer tie tube	Inc-718	0.67818	0.69850
Gap	Hydrogen	0.69850	0.70485
Insulator tube	ZrC (50% TD)	0.70485	0.80645
Gap	Hydrogen	0.80645	0.81280
Hexagonal element body	Graphite	1.89484 cm (0.746 in)*	
Element Exterior cladding	ZrC (100% TD)	0.00508 cm (0.002 in) thick coating	

* Hexagonal element dimension across the flats prior to coating.

Acknowledgments

This work was supported by Prometheus Power and Propulsion at NASA HQ, and by the Department of Energy's Idaho National Laboratory.

References

[1] "The Vision for Space Exploration," NASA NP-2004-01-334-HQ, Feb 2004.

[2] Durham. F. P., "Nuclear Engine Definition Study Preliminary Report, Volume 1 - Engine Description", Los Alamos National Laboratory, Report LA-5044-MS Vol 1, Los Alamos, NM, Sept 1972.

[3] Durham. F. P., "Nuclear Engine Definition Study Preliminary Report, Volume 2 – Supporting Studies", Los Alamos National Laboratory, Report LA-5044-MS Vol 2, Los Alamos, NM, Sept 1972.

[4] Stewart, Mark E. M. and Schnitzler, Bruce G., "Thermal Hydraulic and Structural Analysis of the Small Nuclear Rocket Engine (SNRE) Core", AIAA-2007-5619, July 2007.

[5] Pelaccio, Dennis G., Schiel, Christine M., & Petrosky, Lyman, "Nuclear Engine System Simulation (NESS): Version 2.0", NASA CR-191081, Mar 1993.

[6] Taub, J. M., "A Review of Fuel Element Development for Nuclear Rocket Engines", Los Alamos National Lab., Report LA-5931, Los Alamos, NM, June 1975.

[7] Lyon, L. L., "Performance of (U,Zr)C-Graphite (Composite) and of (U,Zr)C (Carbide) Fuel Elements in the Nuclear Furnace 1 Test Reactor", Los Alamos National Laboratory. Report LA-5398-MS, Los Alamos, NM, Sept 1973.

8 X-5 Monte Carlo Team, "MCNP – A General Monte Carlo N-Particle Transport Code, Version 5", Los Alamos National Laboratory, Report LA-UR-03-1987, Los Alamos, NM, April 2003.

[9] Garber, D., (Editor), "Evaluated Nuclear Data File (ENDF/B-V)", National Nuclear Data Center, Brookhaven National Laboratory Report BNL-17541, October 1975.

[10] McLane, V., Dunford, C. L., and Rose,P. F., (Editors), "ENDF-102, Data Formats and Procedures for the Evaluated Nuclear Data File ENDF-6 (Revised)", Brookhaven National Laboratory Report BNL-NCS-44945, November 1995.

[11] Howerton, R. J., et al., "The LLL Evaluated Nuclear Data Library (ENDL): Evaluation Techniques, Reaction Index, and Descriptions of Individual Reactions", Lawrence Livermore National Laboratory Report UCRL-50400, Volume 15, Part A, September 1975.